

Selection of Single-Walled Carbon Nanotube with Narrow Diameter Distribution by Using a PPE–PPV Copolymer

Yusheng Chen,[†] Andrey Malkovskiy,[‡] Xiao-Qian Wang,[§] Marisabel Lebron-Colon,^{||} Alexei P. Sokolov,[⊥] Kelly Perry,[⊥] Karren More,[⊥] and Yi Pang^{*,†}

[†]Department of Chemistry and [‡]Department of Polymer Science, University of Akron, Akron, Ohio 44325, United States

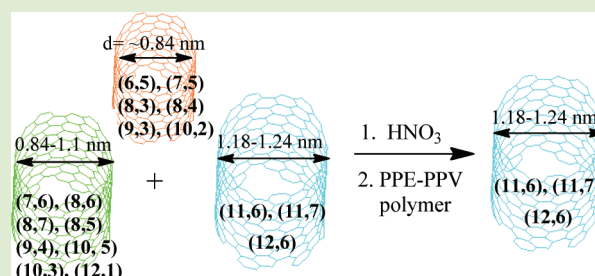
[§]Department of Physics, Department of Chemistry, and Center for Functional Nanoscale Materials, Clark Atlanta University, Atlanta, Georgia 30314, United States

^{||}Structures and Materials Division, NASA Glenn Research Center, Cleveland, Ohio 44135, United States

[⊥]Oak Ridge National Laboratory, Oak Ridge, Tennessee 37831-6197, United States

S Supporting Information

ABSTRACT: Electronic and mechanic properties of single-walled carbon nanotubes (SWNTs) are uniquely dependent on the tube's chiralities and diameters. Isolation of different type SWNTs remains one of the fundamental and challenging issues in nanotube science. Herein, we demonstrate that SWNTs can be effectively enriched to a narrow diameter range by sequential treatment of the HiPco sample with nitric acid and a π -conjugated copolymer poly(phenyleneethynylene) (PPE)–*co*-poly(phenylenevinylene) (PPV). On the basis of Raman, fluorescence, and microscopic evidence, the nitric acid is found to selectively remove the SWNTs of small diameter. The polymer *not only* effectively dispersed carbon nanotubes *but also* exhibited a good selectivity toward a few SWNTs. The reported approach thus offers a new methodology to isolate SWNTs, which has the potential to operate in a relatively large scale.



Since their discovery in 1991,¹ single-walled nanotubes (SWNTs) have attracted much attention due to their superior mechanical,² electrical,^{3,4} and electronic properties that have led to their use in various applications, including flexible electronics,⁵ biosensors,⁶ and transistors.⁷ The electronic structure and optical properties of individual SWNTs are uniquely dependent on the chiral indices (n,m) which separate the tubes into metallic and semiconducting forms.⁸ The chiral indices (n,m) are also equivalently identified by the tube diameter and its chiral angles. In the as-prepared sample, tubes are generally grown as a complex mixture containing many different chiral species. To obtain SWNTs with well-defined chirality, one has to develop an effective methodology to sort different SWNTs. Selective enrichment and individualization of SWNTs play a vital role in the realization of the true application potential of SWNTs.

Separation of a specific tube from a mixture of SWNTs remains a major challenge in the field, as the structural similarity makes it very difficult to differentiate between the different SWNT species.⁹ The chirality of SWNTs can be enriched from a mixture by using proper dispersing reagents, which include an alkyl amine,^{10–12} porphyrin,¹³ pyrene,¹⁴ flavin,¹⁵ and DNA.^{16–19} Isolation of a *specific* chiral (n,m) SWNT from a mixture is dependent on the tube's selective interaction with the dispersing reagents. Recent progress has shown that significant enrichment of selective semiconducting

SWNTs can be achieved by selective interaction of SWNTs with flavin mononucleotide¹⁵ and oligo-DNAs.^{18,19} These methods, however, can only isolate SWNTs in small quantity (e.g., <0.1 mg by using oligo-DNA), which can not meet the demand of studying carbon nanotubes with a preferred structure.

Few chemical reactions are known to be useful in the SWNT purification, although using a selective chemical reaction to remove undesirable components is a classical purification method. Separation of semiconducting from metallic SWNTs can be achieved by using 4-hydroxybenzene diazonium, which selectively reacts with *metallic* SWNTs.²² Deprotonation of the reacted metallic SWNTs by alkaline solution, followed by electrophoretic separation of the charged species, allows us to remove the metallic SWNTs from the unreacted semiconducting SWNTs. Concentrated H₂SO₄/HNO₃ is also reported to selectively react with metallic SWNTs of smaller diameter.²³ Despite its relative poor performance in sorting out individual chiral SWNTs, its ability to operate on a relatively large scale remains to be an attractive feature.

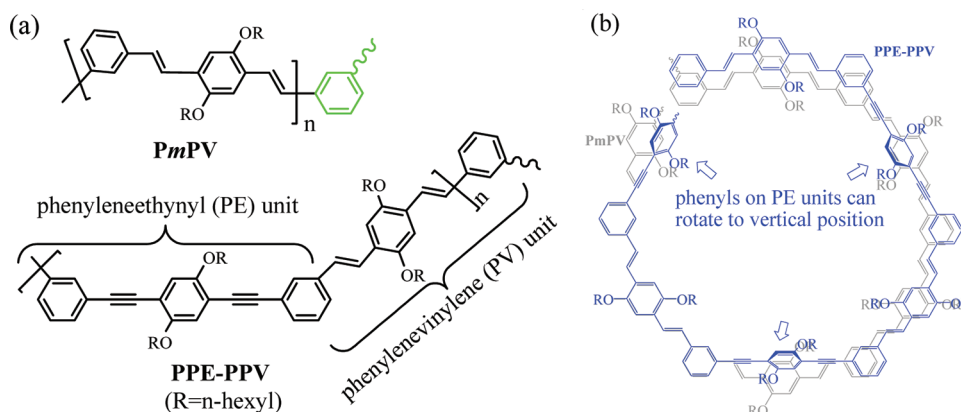
In addition to using small molecular reagents in selective dispersion and reactions, π -conjugated polymers have emerged

Received: October 4, 2011

Accepted: December 23, 2011

Published: December 29, 2011

Scheme 1. (a) Chemical Structures of PmPV and PPE–PPV and (b) Overlay of PmPV (Gray Color) and PPE–PPV (Blue Color) Oligomers in Helical Conformations, Showing That The PPE–PPV Has a Slightly Larger Conformation Cavity^a



^aThe thick arrows point to the phenyl groups that can rotate to a vertical position.

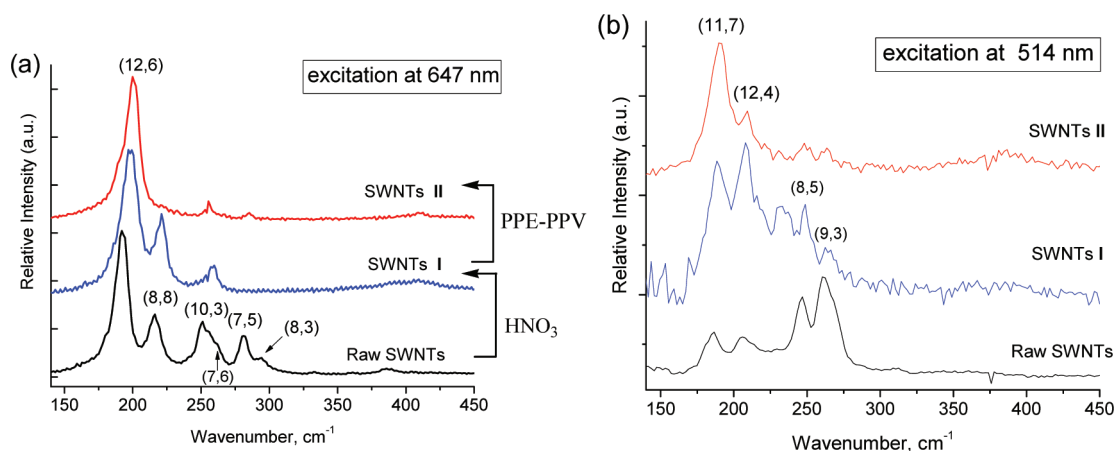


Figure 1. Raman spectra of SWNT samples in the radial breathing mode (RBM) region at 647 nm (a) and 514 nm excitation (b). The as-prepared raw SWNTs are subsequently treated with HNO₃ (SWNTs I) and wrapped by the PPE–PPV polymer (SWNTs II).

as an attractive alternative to achieve the SWNT purification. Currently, polyfluorene has exhibited the potential to differentiate various nanotube species and is capable of enriching the semiconducting (10,5) SWNT to ~60%²⁰ and (7,5) SWNT to ~75% purity.^{24,25} The fluorene-based copolymers have shown improved characteristics in isolating semiconducting SWNTs, achieving enriched (11,3), (9,7), and (10,3) SWNTs with proper chiral side chain²⁶ and leading to near pure (6,5) SWNTs (~90%) with the 2,2'-bipyridinyl group on the main chain.²¹ Selective dispersion of large diameter SWNTs has also been demonstrated recently by degradable²⁷ and photocleavable²⁸ conjugated polymers. Challenges remain in searching for the effective methodologies that have the potential to achieve a large-scale separation. Herein, we demonstrate that a simple treatment with nitric acid leads to unexpected chemical reactivity that selectively removes SWNTs of smaller diameter SWNTs, thereby simplifying the SWNT isolation by having fewer SWNT species. Subsequent treatment of the sample with a conjugated copolymer, i.e., poly(phenyleneethynylene)-*co*-poly(phenylenevinylene) (PPE–PPV)²⁹ (Scheme 1), further narrows the chirality distribution in the sample. Molecular modeling showed that the helical conformation of PPE–PPV had a slightly larger cavity in comparison with that of PmPV.³⁰ In addition, the phenylene in the phenyleneethynylene (PE) units can rotate easily around

the carbon–carbon triple bonds, as their cylindrical orbital shapes lead to a low rotational barrier (0.64–3.3 kcal/mol).^{31,32} These factors allow the molecule to quickly adjust the polymer conformation for intimate interaction with SWNTs of a suitable diameter.

In the first purification step, the raw SWNTs (about 0.5–1 g) prepared from the HiPco process were treated with aqueous HNO₃ (2.6 M, 300 mL) under reflux conditions to afford SWNTs I in ~30% yield.³⁰ Interestingly, the majority of semiconducting SWNTs, including (10,3), (7,5), and (8,3) species, was removed, as observed from Raman spectra (Figure 1a). UV–vis absorption spectra (Figure 2) further confirmed the Raman observations since the nitric acid treated sample SWNTs I revealed much lower absorption between 1050 and 1350 nm which is associated with the semiconducting (7,5) and (8,3) SWNTs.¹⁸ The nitric acid treatment, therefore, selectively removed the SWNTs of smaller diameter: (8,3), (7,5), and (10,3) SWNTs ($d = 0.78, 0.83,$ and 0.93 nm, respectively).^{33,30} The metallic (8,8) and (12,6) SWNTs with respective tube diameters of 1.08 and 1.24 nm, however, were not affected. Raman analysis of the sample series with green laser excitation at 514 nm displayed a consistent pattern (Figure 1b), showing that the nitric acid removed the small-diameter (9,3) and (8,5) SWNTs (with diameter of 0.84 and 0.89 nm, respectively).

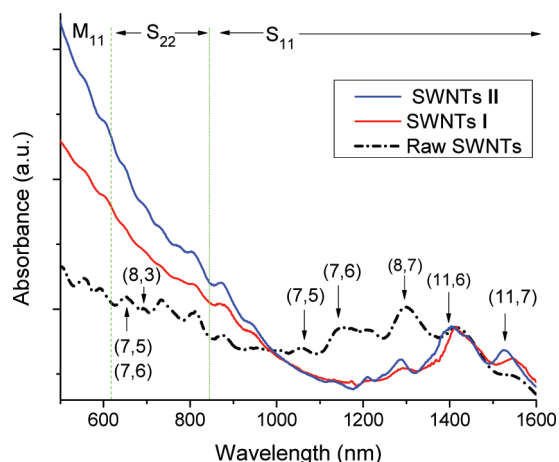


Figure 2. UV-vis absorption spectra of dispersed SWNTs in THF.

High-resolution TEM (Supporting Information, Figure S1) further revealed that nanotubes in SWNTs I were bundled. The tube diameters were found between 1 and 1.2 nm, in agreement with the observation from Raman spectra. The result is in sharp contrast to using concentrated $\text{H}_2\text{SO}_4/\text{HNO}_3$ (ratio 1:9, with 97% H_2SO_4 and 60% HNO_3) at room temperature, which is reported to selectively react with *metallic* SWNTs of smaller diameter (less than 1.1 nm).²³ A possible explanation is that the dilute HNO_3 generated a low concentration of NO_2^+ , which selectively reacted with the small-diameter SWNTs. The observed higher reactivity of the small-diameter SWNTs can be attributed to their increased curvature strain,^{34–36} in comparison with the relative lower reactivity of larger-diameter nanotubes.

The intriguing chemical selectivity of HNO_3 toward different (n,m) SWNTs was further examined by photoluminescence (PL) spectra. Figure 3 shows the 2D-PL mapping of the dissolved SWNTs in THF, where the SWNTs were assigned according to the literature.³³ Nitric acid treatment removed nearly all the small-diameter tubes ($d < 0.9$ nm, see Table 1), including the major semiconducting species (8,4) and (7,6) SWNTs. The result complements the finding from the Raman spectra (Figure 1), demonstrating that the nitric acid selectively reacted with both semiconducting and metallic SWNTs of small diameters.

Selective Polymer Dispersion. The SWNTs I were then treated with PPE-PPV ($M_w = 31\,000$, PDI = 4.6) which was synthesized as described previously.²⁹ In a typical dispersion

Table 1. Distribution of HiPco SWNT Structure and Diameter in the Studied Sample

SWNT structures	tube diameters (nm)	SWNT structures	tube diameters (nm)
(6,5)- <i>sc</i> ^{a,b}	0.757	(10,3)- <i>sc</i>	0.936
(8,3)- <i>sc</i>	0.782	(8,6)- <i>sc</i>	0.966
(7,5)- <i>sc</i>	0.829	(9,5)- <i>sc</i>	0.976
(9,3)- <i>met</i> ^{a,b}	0.84	(8,7)- <i>sc</i>	1.032
(8,4)- <i>sc</i>	0.840	(8,8)- <i>met</i>	1.08
(8,5)- <i>met</i>	0.89	(9,7)- <i>sc</i>	1.103
(10,2)- <i>sc</i>	0.884	(12,4)- <i>sc</i>	1.145
(7,6)- <i>sc</i>	0.895	(11,6)- <i>sc</i>	1.186
(9,4)- <i>sc</i>	0.916	(11,7)- <i>sc</i>	1.248
		(12,6)- <i>met</i>	1.24

^{a,b}the “*sc*” and “*met*” denote *semiconducting* and *metallic* tubes, respectively.

procedure,³⁰ 3 mg of SWNTs I sample and 20 mL of THF were sonicated for 3 h. Then 50 μL of PPE-PPV in THF solution (concn = 26.2 mg/mL) was added to the SWNT suspension, and the mixture was sonicated at 0 °C for an additional 1 h. The supernatant solution was separated from the sediment by centrifugation at 7000g. Raman analysis of the resulting supernatant solution showed that the (12,6) and (11,7) SWNTs I were separated from the (8,8) SWNT (Figure 1). The sediment sample was found to contain an enriched (8,8) SWNT, further confirming the separation. The enriched (11,7) SWNT was also observable from the absorption spectrum (λ_{max} at ~ 1525 nm, Figure 2), where the absorption peak is assigned according to the literature.^{33,37} The absorption band at ~ 1397 nm, which was assigned to (11,6) SWNT ($d = 1.186$ nm),³³ was relatively less affected. 2D fluorescence spectra (Figure 3b,c) revealed that PPE-PPV treatment further purified the sample by selectively removing (8,6) SWNT. Due to the instrument limitations, we were not able to detect the (11,7) SWNT from the fluorescence spectrum since its emission is at ~ 1520 nm (out of the instrument scan range).³³ The results revealed a striking pattern that the reported approach led to a SWNT sample with very narrow distribution of diameter, which is 1.23 and 1.24 nm for (11,7) and (12,6) SWNTs, respectively. The *co*-polymer PPE-PPV thus exhibited good selectivity toward certain SWNT species, in contrast to *Pm*PV which exhibits little selectivity to specific SWNTs.^{30,38} Dispersion of raw SWNTs showed that PPE-PPV also exhibited high selectivity toward the (7,5) SWNT of small diameter, in addition to (12,6) SWNT (Supporting

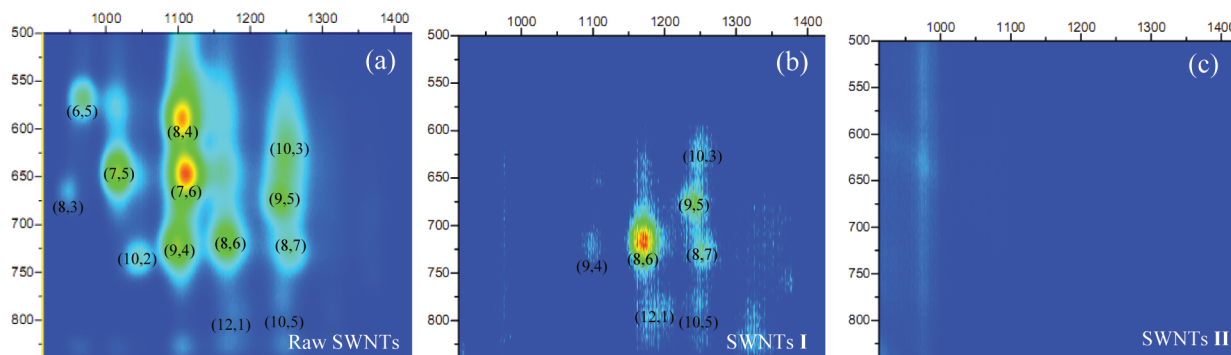


Figure 3. 2D photoluminescence (PL) of SWNT samples in THF (excitation, 500–840 nm; emission, 912–1415 nm). Raw SWNTs were dispersed with addition of sodium dodecylbenzene sulfonate (SDBS) surfactant (65% in water).

Information, Figure S3). Therefore, the treatment with nitric acid was a necessary step.

Raman analysis further revealed that chemical reaction increased the intensity of the D-band due to the reaction on the nanotubes and decreased the intensity for the tangential mode (G-band) due to the loss of electronic resonance (Figure

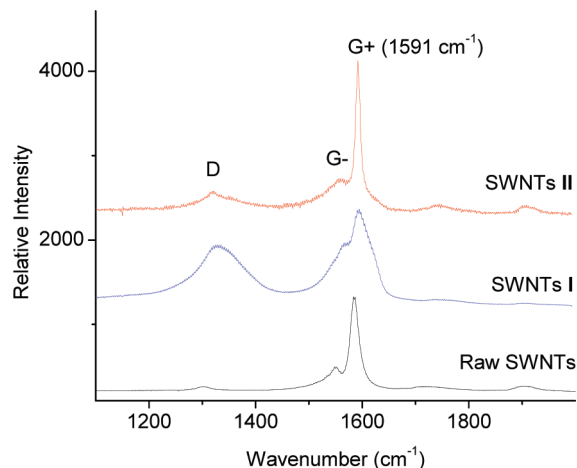


Figure 4. Raman spectra of SWNT samples in tangential mode (G-band) and disorder-related mode (D-band) at 647 nm excitation. The as-prepared raw SWNTs are subsequently treated with HNO_3 (SWNTs I) and wrapped by the PPE–PPV polymer (SWNTs II).

4). Polymer treatment by using PPE–PPV, however, removed those defective tubes of smaller diameters. The result showed that the polymer wrapping was a necessary step in achieving the desirable separation and removing those defective tubes.

An atomic force microscopy (AFM) image of the SWNT/PPE–PPV sample from the supernatant solution revealed that the SWNT sample was dispersed as a single tube (Figure 5). AFM profilometry (in tapping mode) along the lengthwise SWNT direction gave a height profile of regular pattern, indicating that the nanotube was wrapped section by section with multiple polymer chains. From the minimum height of the profile, the diameter of the wrapped nanotube was estimated to be ~ 1.3 nm, which is in agreement with the diameter of 1.24 nm reported for (12, 6) and (11,7) SWNTs. Cross-section measurement across a bare SWNT also determined a similar height (~ 1.27 nm).

The observed narrow selectivity toward the (12,6) and (11,7) SWNTs could be related to the polymer's ability to adopt a suitable helical conformation for intimate polymer interaction with larger-diameter nanotubes. A molecular modeling study showed that a set of the substituents are pointing inward in the natural helical conformation of PmPV (Scheme 1b), which could shield the π -conjugated polymer backbone from intimate contact with the SWNT surface. The configuration can be altered in PPE–PPV because the phenyl rings in the phenyleneethynylene (PE) segments could be rotated easily around the $-\text{C}\equiv\text{C}-$ bond due to its low rotational energy barrier.^{31,32} As a consequence, the phenyl rings in the PE segments can adopt the parallel alignment along the nanotube surface (Figure 6), thereby resulting in a more favorable $\pi-\pi^*$ interaction. The modeling results also showed that the natural conformational cavity from PPE–PPV was sufficiently large to match the size of (12, 6). The results were consistent with the observations that the PPE–PPV had a

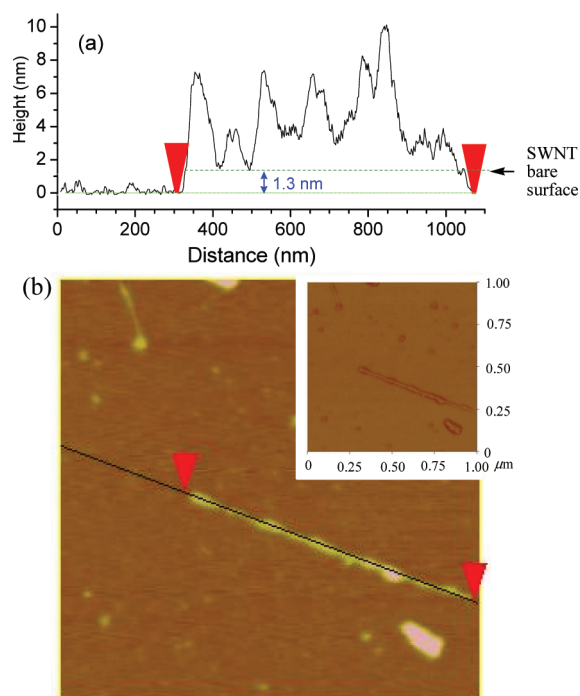


Figure 5. AFM images obtained in tapping mode. (a) A profile along an individual SWNT, where the dashed line shows the 1.3 nm height. (b) Surface images of the SWNT, where the black line indicates the cross-section direction along the tube. The inset image shows the dimension of the same SWNT.

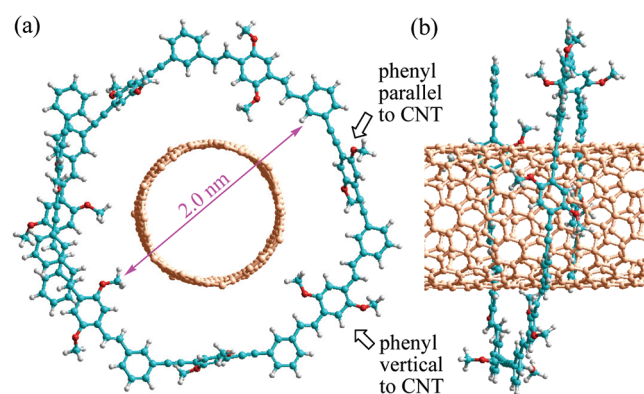


Figure 6. Molecular modeling of the PPE–PPV tetramer ($n = 4$) in front (a) and side view (b), showing a helical conformation with proper cavity size (~ 2.0 nm) to host the (12,6) SWNT. For clarity, the tube is shown in orange color.

favorable interaction with large diameter tubes (12,6) and (11,7) (Figure 1) since those tubes with smaller diameters ($d < 1.14$ nm) would be too loosely fitted into the conformational cavity. The ability of PPE–PPV to adopt a natural helical conformation with enhanced parallel $\pi-\pi^*$ interaction for the SWNT, in addition to proper diameter match, was thought to play a crucial role in the observed selectivity. The assumption was consistent with the finding that the polymer-dispersed SWNTs were in an individual tube (see AFM in Figure 5).

In summary, we have demonstrated that a narrow diameter range of SWNTs, which includes (11,6), (12,6), and (11,7) ($d = 1.18-1.24$ nm), can be isolated by sequential treatment with nitric acid, followed by PPE–PPV polymer wrapping. The nitric acid selectively removed the tubes with small diameters.

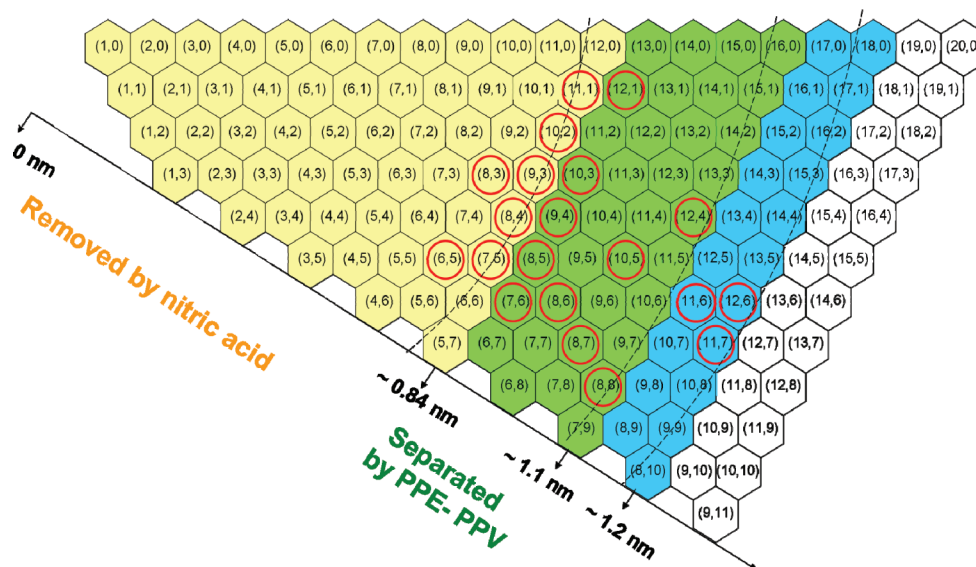


Figure 7. Chirality maps of SWNTs showing that small diameter tubes (yellow color) were removed by HNO_3 , and the remaining SWNTs (green and blue colors) were sorted by PPE–PPV wrapping.

The PPE–PPV polymer can form a unique array in the helical conformation around the SWNTs. Free rotation along a carbon–carbon triple bond allows part of the conjugated backbone to have parallel interaction with SWNT surfaces while retaining the polymer’s natural helical conformation. The helical conformation cavity of PPE–PPV appears to match the diameter of (12,6) ($d = 1.24$ nm) and (11,7) ($d = 1.23$ nm), leading to favorable interaction with SWNTs of specific diameters. The SWNTs can then be released from the wrapping polymer after purification, thereby leading to a useful strategy to access SWNTs of specific diameters for material property studies. The overall diameter-based sorting process can be summarized in Figure 7, where the (n,m) SWNTs in the sample are circled. Nitric acid removed the small diameter tubes (yellow color) selectively, while the remaining SWNTs are sorted into two groups (green and blue colors).

■ ASSOCIATED CONTENT

Supporting Information

Experimental procedures for SWNT dispersion, Raman spectra, and high-resolution TEM images. This material is available free of charge via the Internet at <http://pubs.acs.org>.

■ AUTHOR INFORMATION

Corresponding Author

*E-mail: yp5@uakron.edu.

Notes

The authors declare no competing financial interest.

■ ACKNOWLEDGMENTS

This work was supported by AFOSR (Grant FA9550-10-1-0254). APS acknowledges partial support from the Materials Science and Engineering Division and the SHaRE user Facility, which are sponsored by the Office of Basic Energy Sciences, U.S. Department of Energy.

■ REFERENCES

- (1) Iijima, S. *Nature* **1991**, *354*, 56–58.
- (2) Treacy, M. M. J.; Ebbesen, T. W.; Gibson, J. M. *Nature* **1996**, *381*, 678–680.

- (3) White, C. T.; Todorov, T. N. *Nature* **1998**, *398*, 240–242.
- (4) Ouyang, M.; Huang, J.-L.; Cheung, C. L.; Lieber, C. M. *Science* **2001**, *292*, 702–705.
- (5) Ahn, J.-H.; Kim, H.-S.; Lee, K. J.; Jeon, S.; Kang, S. J.; Sun, Y.; Nuzzo, R. G.; Rogers, J. A. *Science* **2006**, *314*, 1754–1757.
- (6) Kauffman, D. R.; Star, A. *Chem. Soc. Rev.* **2008**, *37*, 1197–1206.
- (7) Lemieux, M. C.; Roberts, M.; Barman, S.; Jin, Y. W.; Kim, J. M.; Bao, Z. *Science* **2008**, *321*, 101–103.
- (8) Meyyappan, M. *Carbon Nanotubes: Science and Applications*; CRC Press: New York, 2005.
- (9) Komatsu, N.; Wang, F. *Materials* **2010**, *3*, 3818–3844.
- (10) Chattopadhyay, D.; Galeska, I.; Papadimitrakopoulos, F. *J. Am. Chem. Soc.* **2003**, *125*, 3370–3375.
- (11) Maeda, Y.; Kimura, S.; Kanda, M.; Hirashima, Y.; Hasegawa, T.; Wakahara, T.; Lian, Y.; Nakahodo, T.; Tsuchiya, T.; Akasaka, T.; Lu, J.; Zhang, X.; Gao, Y.; Yu, Y.; Nagase, S.; Kazaoui, S.; Minami, N.; Shimizu, T.; Tokumoto, H.; Saito, R. *J. Am. Chem. Soc.* **2005**, *127*, 10287–10290.
- (12) Maeda, Y.; Kanda, M.; Hashimoto, M.; Hasegawa, T.; Kimura, S.; Lian, Y.; Wakahara, T.; Akasaka, T.; Kazaoui, S.; Minami, N.; Okazaki, T.; Hayamizu, Y.; Hata, K.; Lu, J.; Nagase, S. *J. Am. Chem. Soc.* **2006**, *128*, 12239–12242.
- (13) Li, H.; Zhou, B.; Lin, Y.; Gu, L.; Wang, W.; Fernando, K. A. S.; Kumar, S.; Allard, L. F.; Sun, Y. P. *J. Am. Chem. Soc.* **2004**, *126*, 1014–1015.
- (14) Wang, W.; Fernando, K. A. S.; Lin, Y.; Meziani, M. J.; Veca, L. M.; Cao, L.; Zhang, P.; Kimani, M. M.; Sun, Y. P. *J. Am. Chem. Soc.* **2008**, *130*, 1415–1419.
- (15) Ju, S. Y.; Doll, J.; Sharma, I.; Papadimitrakopoulos, F. *Nature Nanotechnol.* **2008**, *3*, 356–362.
- (16) Zheng, M.; Jagota, A.; Semke, E. D.; Diner, B. A.; Mclean, R. S.; Lustig, S. R.; Richardson, R. E.; Tassi, N. G. *Nat. Mater.* **2003**, *2*, 338–342.
- (17) Zheng, M.; Jagota, A.; Strano, M. S.; Santos, A. P.; Barone, P.; Chou, S. G.; Diner, B. A.; Dresselhaus, M. S.; Mclean, R. S.; Onoa, G. B.; Samsonidze, G. G.; Semke, E. D.; Usrey, M.; Walls, D. J. *Science* **2003**, *302*, 1545–1548.
- (18) Tu, X.; Manohar, S.; Jagota, A.; Zheng, M. *Nature* **2009**, *460*, 250–253.
- (19) Tu, X.; Hight Walker, A. R.; Khripin, C. Y.; Zheng, M. *J. Am. Chem. Soc.* **2011**, *133*, 12998–13001.
- (20) Nish, A.; Hwang, J.-Y.; Doig, J.; Nicholas, R. J. *Nature Nanotechnol.* **2007**, *2*, 640–646.

- (21) Ozawa, H.; Ide, N.; Fujigaya, T.; Niidome, Y.; Nakashima, N. *Chem. Lett.* **2011**, *40*, 239–241.
- (22) Kim, W. J.; Usrey, M. L.; Strano, M. S. *Chem. Mater.* **2007**, *19*, 1571–1576.
- (23) Yang, C. M.; Park, J. S.; An, K. H.; Lim, S. C.; Seo, K.; Kim, B.; Park, K. A.; Han, S.; Park, C. Y.; Lee, Y. H. *J. Phys. Chem. B* **2005**, *109*, 19242–19248.
- (24) Hwang, J. Y.; Nish, A.; Doig, J.; Douven, S.; Chen, C. W.; Chen, L. C.; Nicholas, R. J. *J. Am. Chem. Soc.* **2008**, *130*, 3543–3553.
- (25) Chen, F.; Wang, B.; Chen, Y.; Li, L. J. *Nano Lett.* **2007**, *7*, 3013–3017.
- (26) Ozawa, H.; Fujigaya, T.; Niidome, Y.; Hotta, N.; Fujiki, M.; Nakashima, N. *J. Am. Chem. Soc.* **2011**, *133*, 2651–2657.
- (27) Wang, W. Z.; Li, W. F.; Pan, X. Y.; Li, C. M.; Mu, Y. G.; Rogers, J. A.; Chan-Park, M. B. *Adv. Funct. Mater.* **2011**, *21*, 1643–1651.
- (28) Lemasson, F.; Tittmann, J.; Hennrich, F.; Sturzl, N.; Malik, S.; Kappes, M. M.; Mayor, M. *Chem. Commun.* **2011**, *47*, 7428–7430.
- (29) Chu, Q.; Pang, Y.; Ding, L.; Karasz, F. E. *Macromolecules* **2003**, *36*, 3848–3853.
- (30) Yi, W.; Malkovskiy, A.; Chu, Q.; Sokolov, A. P.; Colon, M. L.; Meador, M.; Pang, Y. *J. Phys. Chem. B* **2008**, *112*, 12263–12269.
- (31) Saebo, S.; Almolof, J.; Boggs, J. E.; Stark, J. G. *J. Mol. Struct. (THEOCHEM)* **1989**, *200*, 361–373.
- (32) Bothner-By, A. A.; Dadok, J.; Johnson, T. E.; Lindsey, J. S. *J. Phys. Chem.* **1996**, *100*, 17551–17557.
- (33) Weisman, R. B.; Bachilo, S. M. *Nano Lett.* **2003**, *3*, 1235–1238.
- (34) Bahr, J. L.; Yang, J.; Kosynkin, D. V.; Bronikowski, M. J.; Smalley, R. E.; Tour, J. M. *J. Am. Chem. Soc.* **2001**, *123*, 6536–6542.
- (35) Zhou, W.; Ooi, Y. H.; usso, R.; apanek, P.; Luzzi, D.; Fischer, J.; Bronikowski, M.; Willis, P.; Smalley, R. *Chem. Phys. Lett.* **2011**, *350*, 6–14.
- (36) Banerjee, S.; Wong, S. S. *Nano Lett.* **2004**, *4*, 1445–1450.
- (37) The absorption peak of 1525 nm is close to the predicted V1–C1 transition (1516 nm) for (11,7).
- (38) Yi, W.; Malkovskiy, A.; Xu, Y.; Wang, X.; Sokolov, A. P.; Lebron-Colon, M.; Meador, M. A.; Pang, Y. *Polymer* **2010**, *51*, 475–481.